scientific reports

Check for updates

OPEN

Comparative analysis of natural and synthetic surfactant adsorption by quartz minerals: an experimental study

Arash Shirali[1], Mohammad Ebrahimi[1]✉, Abdolhossein Hemmati-Sarapardeh[1,2]✉, Mohammad Ranjbar[3] & Mahin Schaffie[1]✉

The efficacy of surfactant flooding for enhanced oil recovery (EOR) can be considerably diminished by the adsorption of surfactant on reservoir rocks. The primary purpose of this study is to assess the equilibrium adsorption behavior of natural (Ziziphus Spina-Christi, ZSC) and to compare with that of synthetic (Sodium Dodecyl Sulfate, SDS) surfactants onto sandstone (quartz) minerals, which has been rarely reported in the available literature. Such a systematic investigation is beneficial for selecting a proper surfactant in EOR applications. For this purpose, electrical conductivity (EC), ultraviolet–visible spectrophotometry (UV-Vis), and Fourier transform infrared (FTIR) techniques were employed to measure the adsorption of surfactant on quartz minerals. From the results of this study, it can be pointed out that the maximum adsorption of SDS and ZCS on quartz minerals is approximately 3 mg/g and 25 mg/g, respectively. The adsorption rate of both surfactants increased with increasing surfactant concentration up to the critical micelle concentration (CMC). The Langmuir, Freundlich, and Temkin isotherm models were used to predict the experimental data. Based on the experimental findings, the Langmuir isotherm provides a good fit to the experimental data, with coefficients of determination (R^2) of 0.9917 for ZSC and 0.9858 for SDS.

Keywords Adsorption, Natural surfactant, SDS, CMC, Quartz minerals, Adsorption isotherm models

Oil and gas remain the world's primary energy suppliers, despite recent advancements in energy production from renewable sources[1]. As a result of increased extraction from oil reservoirs and a subsequent decrease in reservoir pressure, oil production gradually declines[2]. Consequently, the significance of enhanced oil recovery (EOR) approaches in enhancing oil recovery from reservoirs is highlighted by the growing energy demand[3]. Following the primary and secondary steps of oil recovery, approximately half of the original oil in place (OOIP) remains trapped underground[4–6]. Therefore, tertiary recovery methods (EOR) are used to recover the remaining oil[7,8]. Different EOR techniques can be divided into various groups[9–11]. Chemical EOR (CEOR) has garnered a lot of attention lately[12–21]. Surfactants are favorable chemical additives in EOR applications. By reducing the water/oil IFT and increasing the capillary number, surfactants play a vital role in EOR procedures[22,23]. Numerous studies have been conducted on the wettability alteration, and IFT decrease with anionic, cationic, and nonionic surfactants[24,25]. Several variables influence surfactant efficiency in EOR, including the type of surfactant, concentration, reservoir type, fluid properties, temperature, and salinity[26]. Surfactant adsorption on reservoir rock surfaces occurs through several mechanisms, including electrostatic interactions, hydrophobic interactions, hydrogen bonding, and ion exchange, depending on the surfactant type and mineralogical composition of the rock[27]. In sandstone and quartz-rich systems, parameters such as salinity, pH, and temperature significantly influence these mechanisms by altering surface charge, electrical double layer thickness, and surfactant mobility[28]. In comparison to synthetic surfactants, natural surfactants are less costly and more environmentally friendly. The primary source of natural surfactants is saponins. The natural surface-active substances known as saponins are high-molecular-weight glycosides with detergent properties and the ability to create stable foam in water[29,30]. Recently, researchers have focused on the potential of both natural and synthetic surfactants in EOR

[1]Department of Petroleum Engineering, Shahid Bahonar University of Kerman, Kerman, Iran. [2]Key Laboratory of Continental Shale Hydrocarbon Accumulation and Efficient Development, Ministry of Education, Northeast Petroleum University, Daqing 163318, China. [3]Mineral Industries Research Center, Shahid Bahonar University of Kerman, Kerman, Iran. ✉email: m.ebrahimi7373@yahoo.com; aut.hemmati@gmail.com; hemmati@uk.ac.ir; m.schaffie@uk.ac.ir

applications. Ebrahimi et al.[20] examined the wettability reformation of calcite and dolomite rocks from oil-wet to water-wet conditions using the surfactant sodium dodecyl sulfate (SDS). They claimed that the SDS surfactant adsorbs onto rock surfaces, leading to a modification of the wettability of oil-wet rock surfaces to a water-wet state. The impact of the clay fraction's mineralogical composition on surfactant adsorption has been the subject of recent investigations by various authors[31–33]. Wu et al.[34] investigated static adsorption and dynamic adsorption of SDS with and without silica nanoparticles (SNPs). According to the results of this study, it was noted that the addition of SNPs reduces surfactant adsorption on rock.

Herawati et al.[35] studied the adsorption of an anionic alkyl ethoxy carboxylate surfactant on sandstone containing Ca-montmorillonite and kaolinite clays and its effect on wettability alteration. They demonstrated that surfactant adsorption is strongly dependent on clay mineralogy and electrostatic interactions, with higher adsorption resulting in enhanced water-wet conditions.

Belhaj et al.[36] studied the adsorption of an alkyl ether carboxylate and alkyl polyglucoside surfactant mixture on sandstone in the presence and absence of crude oil. They showed that adsorption increases due to surfactant partitioning into oil, emphasizing the importance of considering partitioning effects in surfactant flooding design. In another study, Belhaj et al.[37] investigated surfactant adsorption studies, considering laboratory testing, modeling, and simulation studies. They stated that numerous factors, including surfactant concentration, pH, salinity, temperature, and the mineral composition of the rock, can influence surfactant adsorption.

Belhaj et al.[38] conducted a comprehensive experimental and modeling study on the adsorption behavior of anionic and nonionic surfactants on sandstone under reservoir conditions. Their results demonstrated that surfactant adsorption is governed by heterogeneous mono- and multilayer mechanisms and is strongly affected by temperature, surfactant type, and competitive adsorption in binary systems. In addition, advanced modeling approaches, including adsorption isotherms and artificial neural networks, were shown to be effective tools for predicting surfactant losses and improving surfactant flooding design.

Lebouachera et al.[39] investigated the SDS adsorption on Algerian rock reservoirs. They suggested that reducing surfactant adsorption could lead to improved oil recovery. The adsorption of Ziziphus Spina-Christi (ZSC) surfactant on carbonate minerals was experimentally investigated by Ahmadi and Shadizadeh[40]. In another study, Zendehboudi et al.[41] investigated the equilibrium and kinetic behaviors of ZSC adsorption onto carbonate rock specimens. The findings of their study demonstrated that ZSC considerably reduces the oil-water IFT. The adsorption of surfactants on the minerals leads to the reduction of IFT, the improvement of wettability, and ultimately the mobility of the oil[42]. The adsorption of surfactant may be impacted by the characteristics of the rock surface[20]. Additionally, excessive salinity causes greater adsorption of surfactants[43,44]. The adsorption of surfactants on reservoir rocks reduces their concentration in the liquid phase, which can lead to a decrease in the effectiveness of the surfactant, potentially impacting processes such as oil recovery[45–48]. Surfactant adsorption directly influences its availability at the oil–water interface and therefore governs the extent of interfacial tension (IFT) reduction and wettability alteration in surfactant flooding processes[49–51]. Excessive adsorption on rock surfaces reduces the effective surfactant concentration in the aqueous phase, which can limit capillary number enhancement and ultimately diminish oil recovery efficiency[52,53]. To improve the optimum selection of surfactants for EOR operations, this study aims to perform a comparative analysis of the adsorption of Ziziphus Spina-Christi (ZSC) surfactant (as a natural surfactant) and Sodium Dodecyl Sulfate (SDS) surfactant (as a synthetic surfactant) by sandstone (quartz) minerals. In this regard, various analysis methods, including electrical conductivity (EC), ultraviolet-visible spectrophotometry (UV-Vis), and Fourier transform infrared (FTIR) tests, are used. This study offers further understanding of the applicability of surfactant flooding in reservoir rock systems such as sandstone and contributes valuable data to the advancement of efficient and safe surfactant-based enhanced oil recovery methods. To the best of our knowledge, systematic equilibrium adsorption evaluation of ZSC on sandstone systems and its comparison with SDS under identical experimental conditions has rarely been reported in the literature. Therefore, such direct comparison under identical conditions provides new insights into the feasibility of replacing synthetic surfactants with environmentally friendly natural alternatives in EOR applications.

Materials and methods

Figure 1 illustrates the schematic presentation of research steps. Experiments were conducted with two replicates, and the results presented are the average of the obtained data.

2.1. Adsorbent

In this study, a quartz rock specimen is used as an adsorbent. A jaw crusher was used to disintegrate rock specimens into small pieces, and then they were ground using a rock pulverizer and sieved (Model Azmoontes SO410) through 60- and 80-mesh screens. Then, equal amounts were mixed in a 1:1 ratio and used as an adsorbent. After repeatedly washing the powdered rock specimens with distilled water (DW), they were allowed to settle and decant for 24 h to reduce clay content. Following the reduction of the clay content, the remaining wet quartz particles were dried for 24 h at 100 °C[54,55]. To determine the surface area for adsorption, a Brunauer-Emmett-Teller (BET) test (Model BELSORP Mini II) was performed. Before BET analysis, the quartz samples were degassed under vacuum at 150 °C for 8 h. Nitrogen adsorption–desorption measurements were carried out at 77 K using Nitrogen (N_2) as the adsorbate gas. The specific surface area was calculated using the BET method in the relative pressure range of 0.05–0.30, while pore volume and average pore diameter were determined using the Barrett-Joyner-Halenda method from the desorption branch of the isotherm. The BET analysis and other characteristics of the adsorbent specimen are shown in Table 1, and the results of the X-ray fluorescence (XRF) test are presented in Table 2.

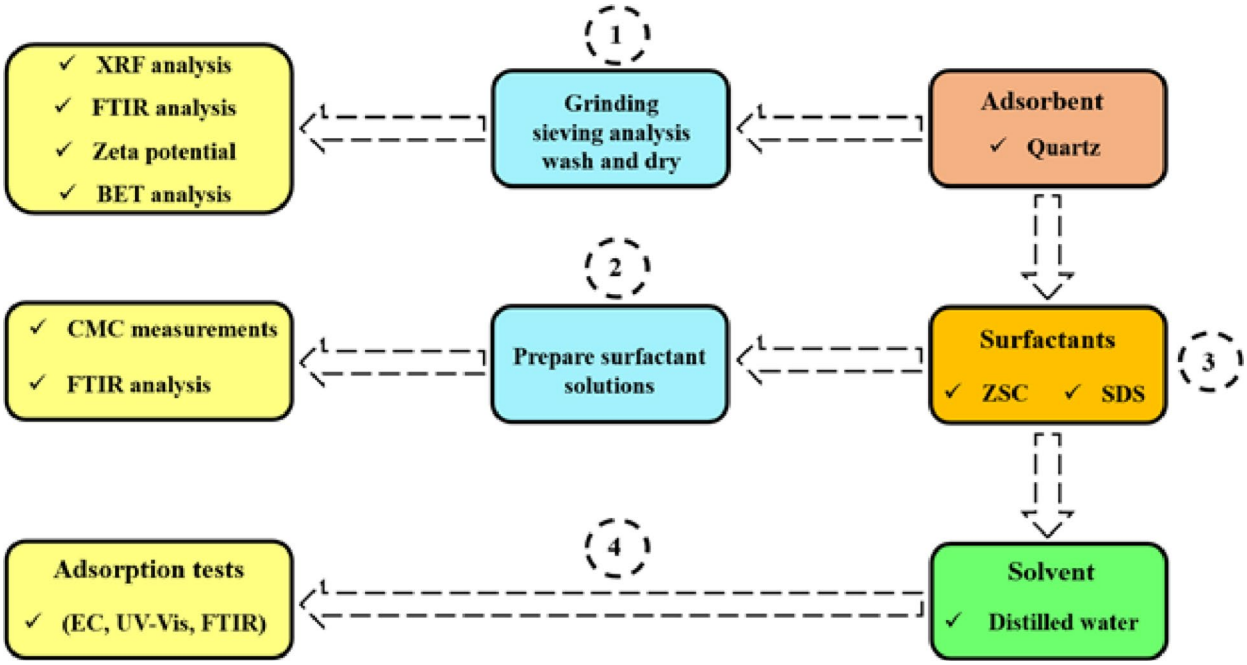

Fig. 1. Schematic of the research steps.

Mineral	Particle size (μm)	Average pore diameter (nm)	Specific surface area (m^2/g)	Pore volume (cm^3/g)
Micro-quartz	170–250	6.0391	5.1874	1.1918

Table 1. The BET analysis results of the adsorbent specimen.

Element	Amount (%)	Element	Amount (%)
SiO_2	79.31	P_2O_5	< 0.01
Al_2O_3	9.9	SO_3	0.18
BaO	0.04	TiO_2	0.11
CaO	0.98	Cr_2O_3	0.01
Fe_2O_3	2.76	Cu	0.06
K_2O	3.29	Pb	< 0.01
MgO	0.38	Zn	< 0.01
MnO	0.04	LOI*	0.79
Na_2O	2.15		

Table 2. The XRF results of quartz. Note: *; loss on ignition.

Surfactants

The synthetic anionic sodium dodecyl sulfate (SDS) and the natural surfactant called Ziziphus Spina-Christi (ZSC) with high concentration of saponins were employed in this study. It should be noted that extracts obtained from ZSC are complex natural mixtures rather than single purified compounds. Although saponins constitute the main surface-active components responsible for interfacial tension reduction, foaming, and adsorption behavior, the extract may also contain sugars, phenolic compounds, organic acids, and inorganic salts. Detailed compositional studies of ZSC leaf extracts have shown that they contain multiple structurally diverse triterpenoid saponins identified by chromatographic and spectroscopic methods, confirming the complex, saponin-rich nature of the extract used in this study[56]. Therefore, the term 'saponin-rich surfactant' is used throughout this study to reflect the dominant role of saponins while acknowledging the multicomponent nature of the extract. Triterpenoid saponins reported for ZSC generally possess molecular weights in the range of approximately 600–1200 g/mol, depending on the aglycone structure and sugar moieties[57,58]. It is worth noting that for the ZSC surfactant, all reported concentrations refer to the total extract concentration. The CMC, adsorption, and conductivity results therefore represent the effective macroscopic behavior of a saponin-rich natural surfactant system rather than that of a single purified compound. ZSC was selected because it is locally abundant, low-cost,

non-toxic, and traditionally recognized as a rich source of triterpenoid saponins with strong surface activity[30,59]. In addition, its availability and ease of extraction make it an attractive candidate for practical, field-scale applications compared with many other plant-based surfactants.

The molecular structure of SDS and ZSC surfactants was presented in[60,61]. Saponin is known as a biosurfactant[40]. SDS, with a density of 1.1 g/cm^3 and a purity of ≥ 86%, was purchased from Merck. Utilizing a magnetic stirrer (Model Alpha D-500), SDS surfactant solutions were prepared at concentrations of up to 2500 ppm in distilled water. The maceration method was used to extract cedar leaves (i.e., ZSC)[59]. For this purpose, 400 g of ZSC powder was mixed with distilled water and stirred for three days. It is worth noting that the process of soaking the cedar leaves at room temperature was performed. After 3 days, the concentrated extract was obtained by filtration and heating of the mixture[59]. The leaves of the cedar tree were used as the plant material in this study. They were commercially purchased from a local market. The material was initially a natural detergent product. The procurement of the plant material was made by the supervisor of the study. The species of the plant was identified by its commercial name and the features that the supplier provided. Since the plant material was obtained from a commercial source and no plants were collected from the wild, no collection permits were necessary, and no voucher specimen was deposited.

In this regard, test solutions were prepared with ZSC surfactant at concentrations of up to 4000 ppm. Adsorbent specimens and surfactant solutions with a ratio of 1:10 (i.e., 1 g of crushed quartz specimen and 10 mL of each solution) were mixed with a magnetic stirrer. The CMC of surfactants was determined by the EC procedure described in[62,63]. All experiments were conducted at ambient pressure and temperature. All surfactant solutions were prepared using distilled water to establish controlled and comparable baseline conditions for comparative analysis. The influence of pH and ionic strength on surfactant adsorption is acknowledged and will be addressed in future studies under reservoir-relevant conditions.

Absorption calibration curve

UV–Vis spectrophotometry was used to determine the surfactants concentrations[19,64]. By plotting absorbance against concentration, a calibration curve was generated. Thus, this process ultimately resulted in the creation of calibration curves and the equations of the best-fit trend lines from the measured data points (Fig. 2).

FTIR analysis

Utilizing a Bruker TENSOR 27 spectrometer, FTIR tests were conducted with 32 scans and a resolution of 4 cm^{-1} in the wavelength range of 400–4000 cm^{-1}. To produce tablets, the different quartz samples were mixed with potassium bromide powder in a 1:100 ratio[65]. This analysis is a qualitative method used to identify functional groups and confirm adsorption[20,66,67]. It is worth noting that all spectra were subjected to baseline correction using the instrument software, and no normalization or difference spectra were applied.

Adsorption study

Adsorption tests were performed to assess the amount of surfactant adsorbed onto quartz. The ratio of solid to liquid weight was 1:10. Known weights of quartz specimens (1 g) were added to 10 mL of ZSC and SDS surfactant solutions at different concentrations. Then, ZSC and SDS solutions with quartz minerals were equilibrated in appropriate vessels with a magnetic stirrer[68,69]. It is worth noting that the maximum adsorption of SDS on quartz is obtained after 45 min, and in the case of saponin-rich extract/quartz, after nearly 83 min. However, in both cases, 150 min was selected as the adsorption time. After that, the specimens were centrifuged at 3800 rpm for 15 min. Then, supernatants were separated and examined for remaining surfactant concentrations. Surfactant adsorption was determined using Eq. (1)[55].

$$q = \frac{m_{solution} \times (c_0 - c)}{m_{absorbent}} \times 10^{-3} \quad (1)$$

where q is the surfactant adsorption rate on absorbent surfaces (mg/g-absorbent), $m_{solution}$ is the total mass of solution in the original bulk solution (g), C_o is surfactant concentration in the initial solution (ppm), c denotes surfactant concentration in aqueous solution after adsorption (ppm), and $m_{absorbent}$ is the total mass of the quartz minerals used (g).

Results and discussion

Zeta potential determination

Figure 3 shows the results of the zeta potential analysis for the quartz used in this study. The maximum zeta potential for quartz is −45 mV. The surface charge for quartz is negative and is comparable to values reported in existing references for sandstone minerals[20,70].

FTIR analysis

Qualitative assessment of surfactant adsorption on adsorbent surfaces is performed using FTIR analysis (Fig. 4). The absorption band at 489.44 cm^{-1} corresponds to the asymmetric bending vibration of the Si-O bond[71]. The symmetric and asymmetric vibrations of the Si-O bond are represented by peaks located at 768.24 cm^{-1} and 1133.13 cm^{-1}, respectively[72]. The O-H bond was identified at a wavenumber of 3626.27 cm^{-1}[73]. Therefore, the rock consists of pure silica as the primary component of quartz.

Determination of CMC

When saponins are dispersed into aqueous solutions, they self-assemble into micellar aggregates[74]. A conductivity device was used to measure the conductivity of the solutions. To obtain the CMC, the data were plotted as a

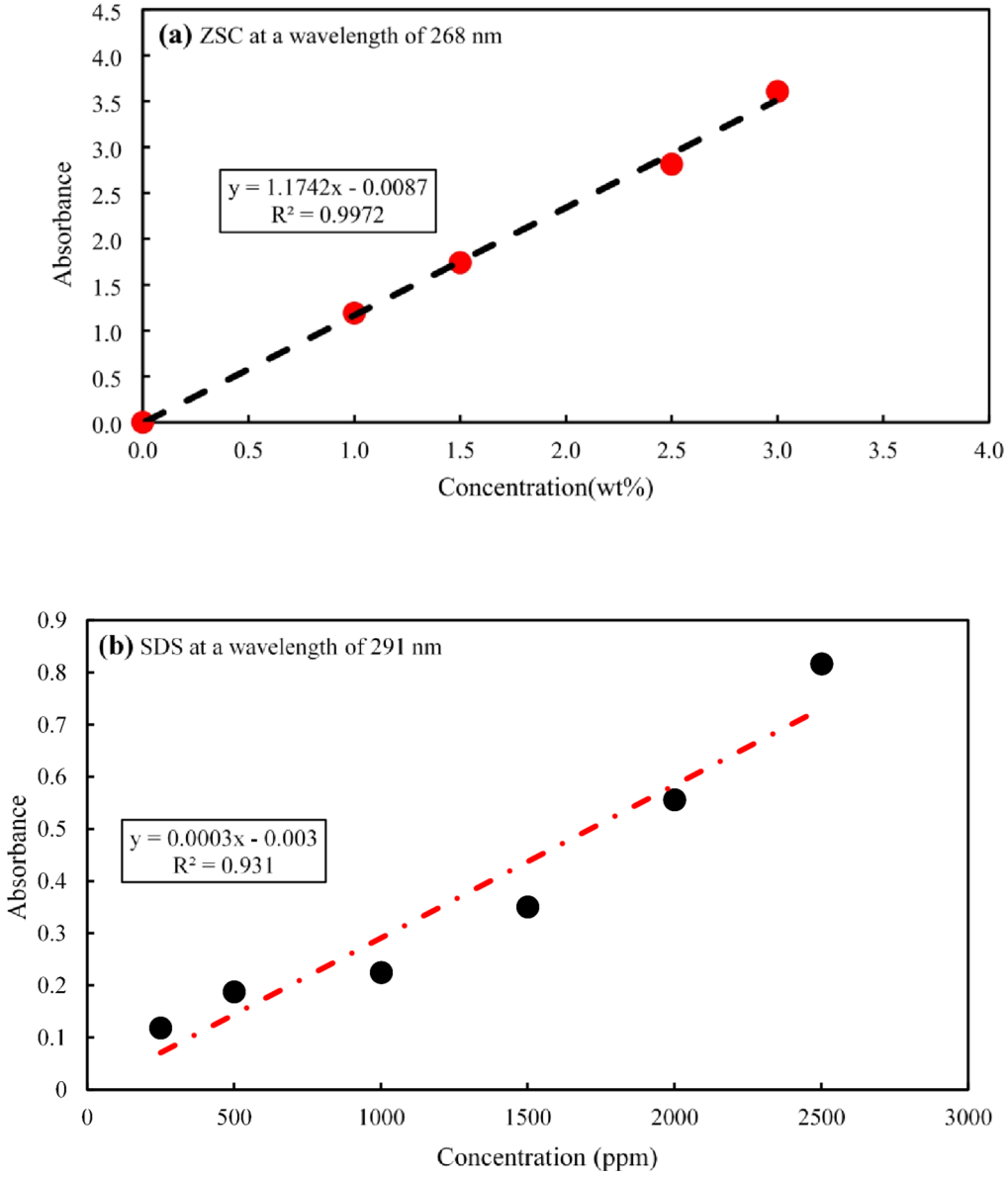

Fig. 2. Calibration curve of surfactant specimens (a) ZSC and (b) SDS.

graph of conductivity versus concentration, and the value of CMC was determined from the inflection point in the curve[75]. According to the results presented in Fig. 5, the intersection of the two lines indicates the CMC concentration, which is about 2007 ppm for the SDS and around 36,614 ppm for the ZSC surfactant. The relatively high CMC value obtained for ZSC reflects the use of a crude saponin-rich extract. Therefore, the CMC of Ziziphus Spina-Christi should be interpreted based on total extract concentration rather than the intrinsic CMC of purified saponin molecules.

Adsorption tests

The amount of surfactant adsorption on the quartz minerals was measured through adsorption studies using conductivity methods and UV spectroscopy at varying concentrations. Figure 6(a) illustrates the amounts of SDS as a function of the equilibrium surfactant concentrations using two analysis methods, and Figs. 6(b) and (c) illustrate the amounts of ZSC and SDS using the UV-Vis spectrophotometry method. In the early steps, the rate of surfactant adsorption is high due to a high accessible adsorption surface[76]. Subsequently, when the available surface area is covered, this rate decreases[77]. At low concentrations of surfactant, surfactant can adsorb as monomers[78]. The measured negative zeta potential of quartz (− 45 mV) indicates that the mineral surface is negatively charged under the experimental conditions. Therefore, adsorption of anionic SDS occurs despite electrostatic repulsion and is mainly attributed to non-electrostatic mechanisms such as hydrophobic association and van der Waals interactions[20,52,79], whereas the amphiphilic saponin molecules in ZSC can additionally interact through hydrogen bonding with surface silanol groups, leading to higher adsorption[80–82]. In other words, the substantially higher adsorption of ZSC compared with SDS can be attributed to the multicomponent,

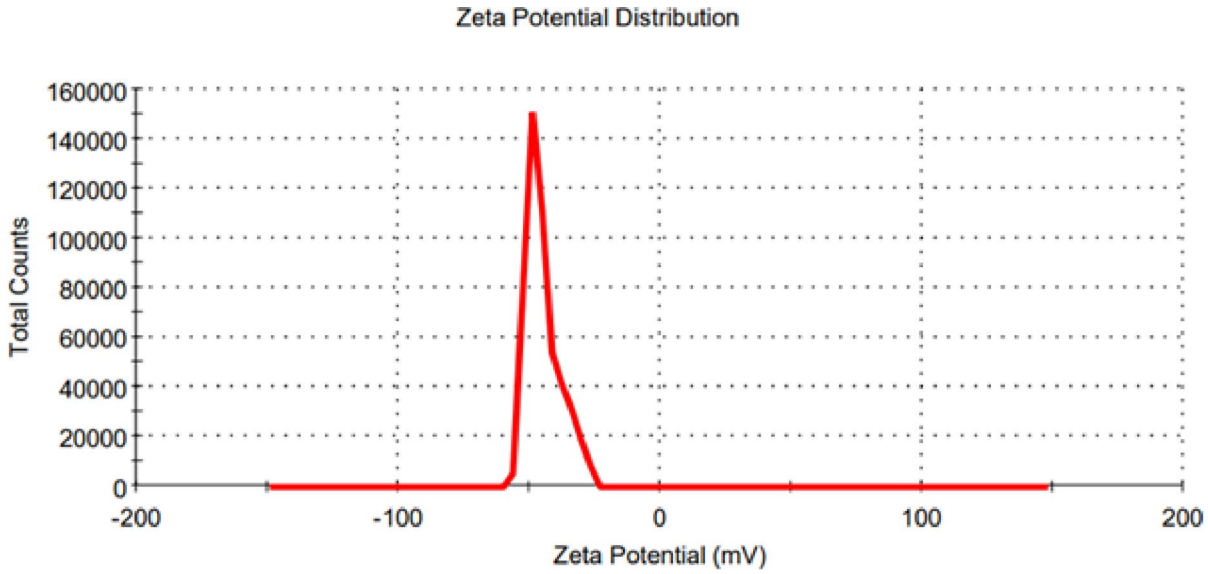

Fig. 3. Zeta potential analysis of pure quartz minerals.

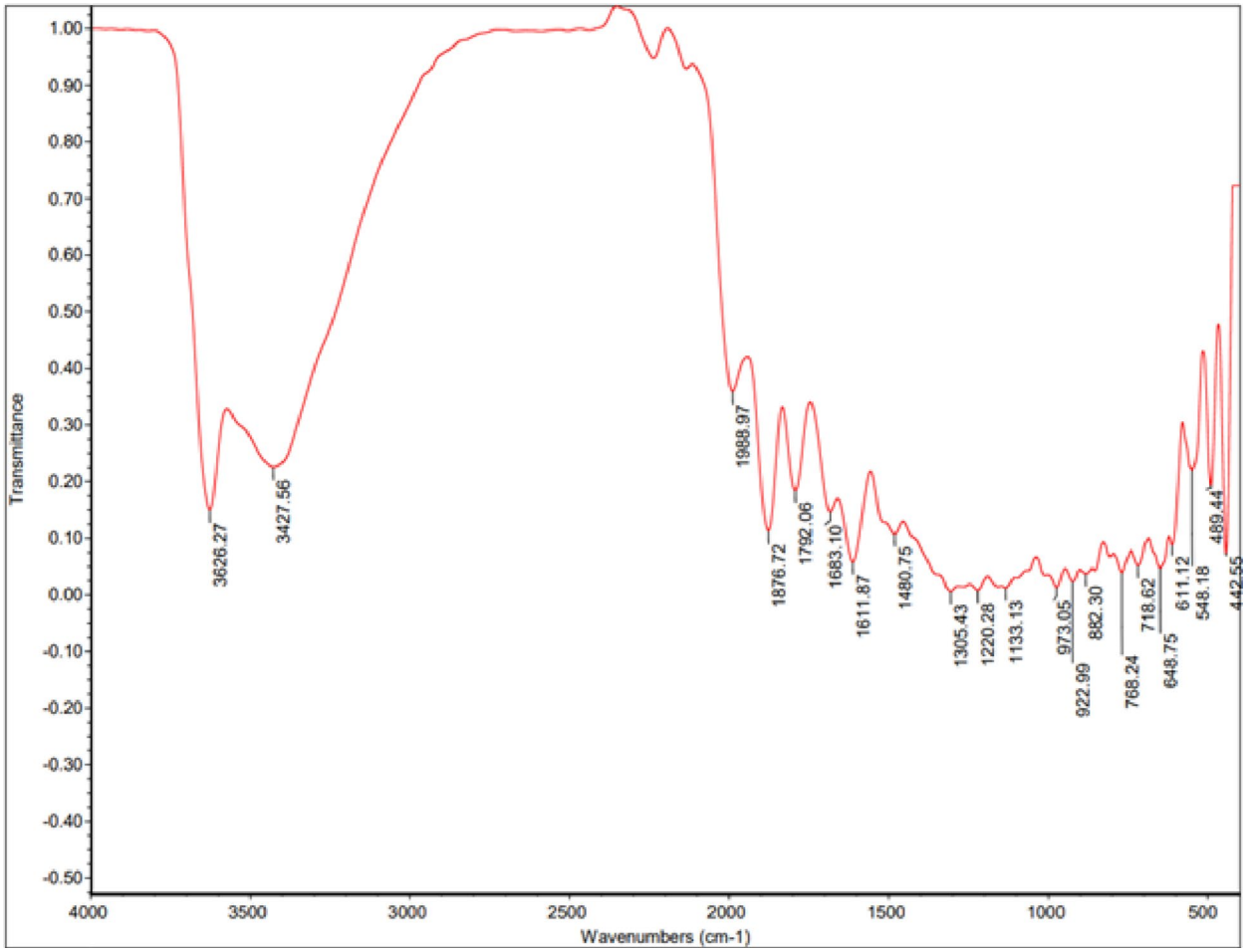

Fig. 4. FTIR analysis of pure quartz.

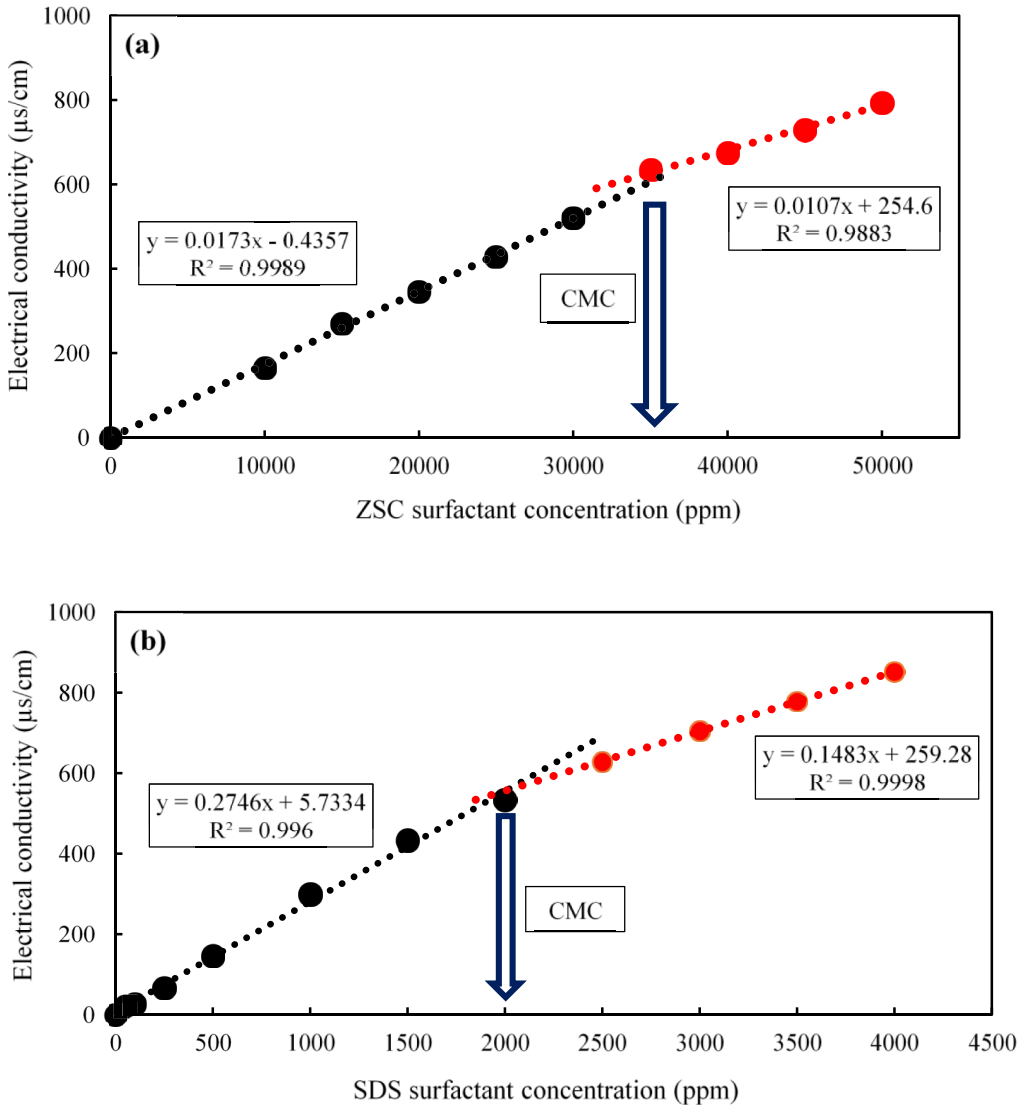

Fig. 5. CMC determination: (a) ZSC and (b) SDS.

triterpenoid-saponin structure of ZSC, which contains multiple hydroxyl groups and sugar moieties capable of strong hydrogen bonding and multisite surface attachment on quartz, in addition to hydrophobic association[83]. Although ZSC showed higher adsorption than SDS, this may limit its direct application in CEOR because of increased surfactant loss. However, previous studies have demonstrated that adsorption of natural and synthetic surfactants can be significantly reduced by the addition of alkali or nanoparticles through competitive adsorption and surface charge modification[34,84]. At elevated concentrations, surfactant molecules begin to aggregate and form hemi-micelles[78]. At surfactant concentrations above the CMC, most active sites on the surface are adsorbed by surfactant molecules, while additional surfactant forms micelles that are repelled by the adsorbed layer[46]. This trend is evident in Fig. 5, where the plot shows a steep slope up to the CMC, followed by a decrease in slope at concentrations above the CMC. In saponin-based substances, hydroxyl groups stick to surface particles via hydrogen bonds[80–82].

It is important to note that reservoir conditions differ significantly from ambient laboratory conditions. Elevated temperature and pressure, as well as high salinity, can alter surfactant adsorption behavior and interfacial properties. Temperature increases have been reported to reduce surfactant adsorption in many systems due to weakened binding interactions and changes in surfactant solubility, and surfactants that are not thermally stable may undergo degradation or loss of activity under reservoir conditions (e.g., high temperatures > 100 °C)[85–87]. Pressure variations may also influence surfactant behavior, although their effects are typically smaller compared to temperature[88]. These factors should be considered in future studies for comprehensive evaluation under realistic reservoir environments.

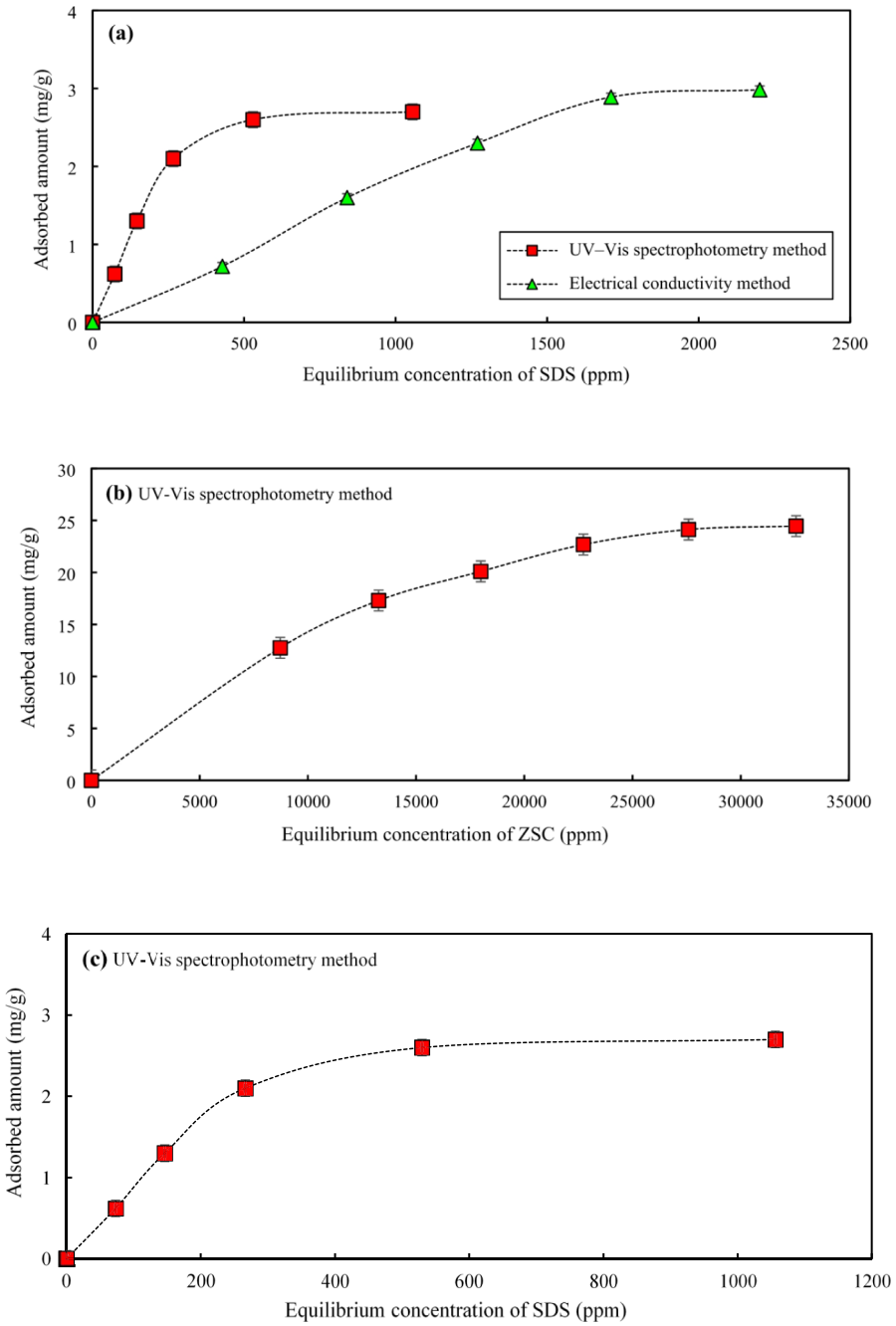

Fig. 6. Adsorption isotherms of SDS and ZSC on quartz using two analysis methods.

FTIR analysis of adsorption

To detect the functional groups, the FTIR analysis was used. Figures 7 and 8 display the FTIR spectra of quartz adsorbent before and after adsorption with SDS and ZSC. The functional groups of the SDS surfactant are displayed in Fig. 7(a). Additionally, Fig. 7(b) illustrates pure quartz, while Fig. 7(c) displays quartz after SDS adsorption. The FTIR spectrum bands for SDS demonstrated distinct peaks at the 3462.46 cm^{-1} (– OH stretching), 2900, and 2841 cm^{-1} (– CH_2 stretching and bending modes), the 1208 cm^{-1} (S = O stretching), and the 800 and 400 cm^{-1} (asymmetric C–H bending of the CH_2 group)[39,89]. Note that the FTIR analysis for pure quartz was done earlier in Fig. 4. In Fig. 7(c), new peaks (red circle) have appeared in comparison to the pure quartz, indicating the adsorption of SDS onto the quartz adsorbent. In other words, after adsorption onto quartz, the spectrum is essentially a superposition of the quartz and SDS spectra. Crucially, there is no significant shift in the wavenumber of the key SDS functional group bands, particularly the S = O stretching band at ~ 1208 cm^{-1}. The absence of a notable change in the characteristic bands of the surfactant indicates that the chemical structure of SDS remains unchanged upon interaction with the quartz surface. The adsorption likely occurs via physical interactions such as electrostatic attraction between the anionic sulfate group (SO_4^{2-}) of SDS and positively

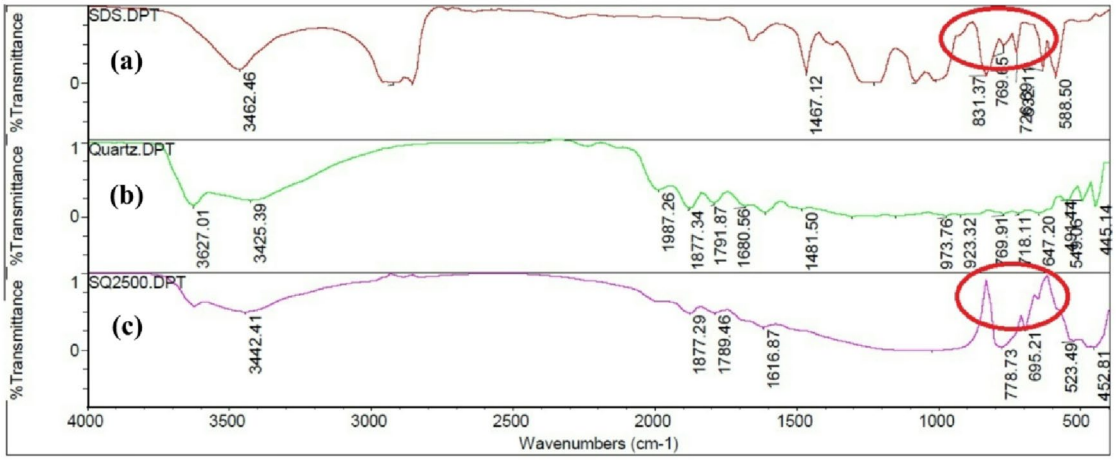

Fig. 7. FTIR analysis of (a) SDS surfactant, (b) pure quartz, and (c) quartz after SDS adsorption.

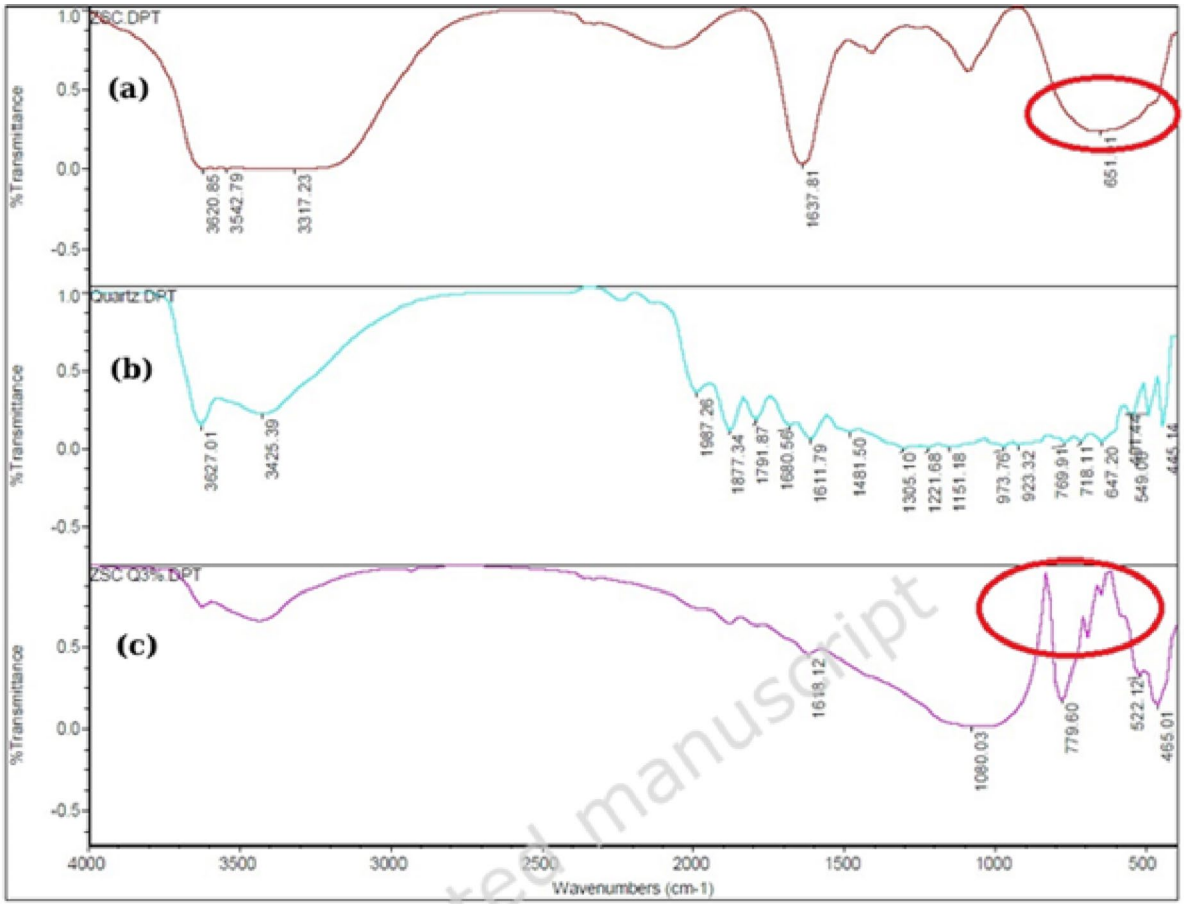

Fig. 8. FTIR analysis (a) ZSC surfactant, (b) pure quartz, and (c) quartz after ZSC adsorption.

charged sites on the quartz surface (e.g., Si-OH_2^+), and/or van der Waals forces between the hydrocarbon tail and the surface[90].

Figure 8 displays the functional groups of pure quartz, ZSC surfactant, and quartz after ZSC adsorption. The ZSC/FTIR spectrum at 3317.23 cm^{-1} is attributed to the hydroxyl group. The band appearing at 1637.81 cm^{-1} is attributed to the formation of oxygen functional groups like C = O stretching in carboxylic groups. The peak at 651 cm^{-1} is caused by C-N-C. A peak at 3542.79 cm^{-1} that is dominated by -NH stretching and illustrates the existence of hydrogen-bonded -OH stretching from alcohol and phenols. The saponin's FTIR spectrum validates

its efficacy as a surface-active species and is mostly in agreement with the literature[91,92]. Figure 8(c) indicates quartz after ZSC adsorption. In Fig. 8(c), new peaks (red circle) have appeared compared to the pure quartz, indicating the adsorption of ZSC onto the quartz adsorbent. The changes in the hydroxyl (-OH) and amine (-NH) regions are particularly significant. Quartz surface is rich in silanol groups (Si-OH). The -OH and -NH groups in ZSC saponins can form strong hydrogen bonds with these surface Si-OH groups. While hydrogen bonding is a stronger specific interaction than van der Waals forces, it is generally still classified under physical adsorption[93]. However, if the interaction leads to the formation of a covalent-like bond, it could indicate chemisorption[93]. The current FTIR evidence does not conclusively indicate chemisorption (covalent bond formation).

Adsorption isotherm models

The large number of isotherm models provided by Kalam et al.[94] and Liu et al.[95] are typically used to modify surfactant adsorption curves. In this study, three well-known adsorption models were applied.

Langmuir isotherm

The Langmuir isotherm model relies on three key assumptions: adsorption occurs in a single monolayer, all adsorption sites are uniform, and each sorption site possesses the same energy. The Langmuir equation can be represented as follows[39,41].

$$q_e = \frac{q_m k_l c_e}{1 + k_l c_e} \tag{2}$$

In this context, $q_e$represents the amount of adsorbed component (mg/g), $q_m$denotes the maximum amount of adsorbed component (mg/g), $k_l$refers to the Langmuir constant (L/mg), and $c_e$indicates the equilibrium concentration (ppm). Equation (2) can be expressed as follows in its linearized form:

$$\frac{1}{q_e} = \frac{1}{q_m} + \frac{1}{k_l q_m c_e} \tag{3}$$

If the adsorption equilibrium values followed the Langmuir isotherm, a linear graph of $1/q_e$ vs. $1/c_e$ will be generated. The slope and intercept of the straight line can be used to obtain the $q_m$and $k_l$amounts, respectively. The fitting of the ZSC and SDS adsorption isotherms using the Langmuir model is shown in Fig. 9. The equilibrium parameter, R_L[39], can be used to express the key features of the Langmuir isotherm. It is defined as follows:

$$R_L = \frac{1}{1 + k_l c_0} \tag{4}$$

Here, c_0 is the initial concentration of the surfactant solution, and k_l is the Langmuir constant. According to the R_L values, the isotherm type can be classified as unfavorable ($R_L > 1$), linear ($R_L = 1$), favorable ($0 < R_L < 1$), or irreversible ($R_L = 0$)[39].

Freundlich isotherm

According to the Freundlich isotherm, multilayer adsorption occurs onto a heterogeneous surface[96,97]. This model is represented by the equation that follows[60]:

$$q_e = k_f c_e^{\frac{1}{n}} \tag{5}$$

where k_f represents the Freundlich isotherm constant and $1/n$ represents the heterogeneity factor. Equation (5) can be displayed in its linear form as follows:

$$\log q_e = \log k_f + \left(\frac{1}{n}\right) \log c_e \tag{6}$$

k_f and n were obtained from the slope and intercept of the linear $\log q_e$ versus $\log c_e$ graph. The fitting of the ZSC and SDS adsorption isotherms using the Freundlich equation is shown in Fig. 10.

Temkin isotherm

The impact of the interaction between the adsorbent and adsorbate molecules is explained by the Temkin isotherm model[78]. The Temkin isotherm recommends that the adsorption heat decreases linearly with increasing coverage[60]. The Temkin equation is represented in the following form[41]:

$$q_e = \frac{RT}{b} \ln (k_t c_e) \tag{7}$$

The simple linear form of the equation above is as follows:

$$q_e = B \ln k_t + B \ln c_e \tag{8}$$

where $B = RT/b$, b and k_t correspond to Temkin constants, T denotes the temperature, and R represents the gas constant. Therefore, linear plotting of q_e versus lnc_e enables one to determine k_t and B from the intercept and

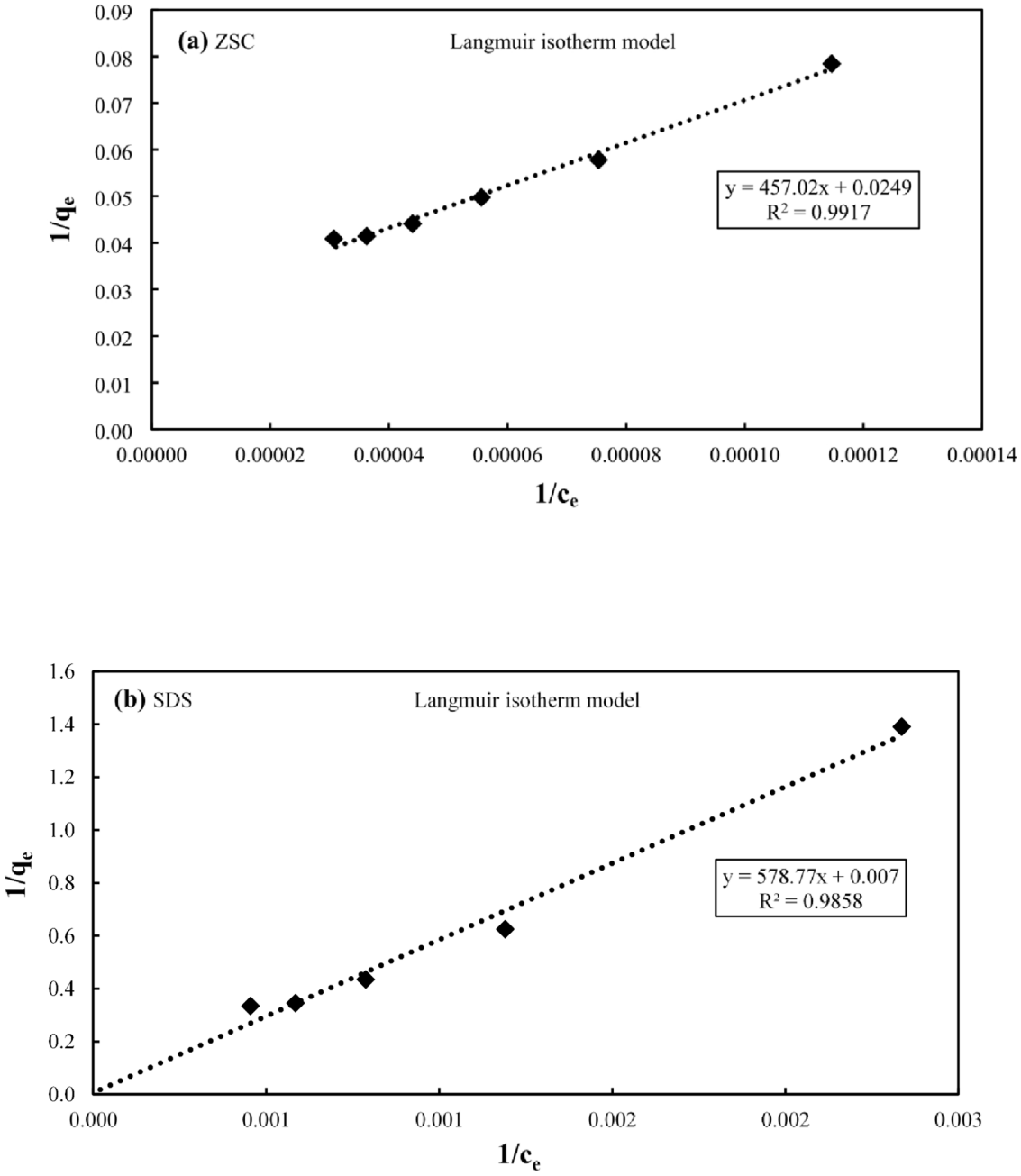

Fig. 9. Langmuir adsorption isotherms fitting curves for (a) ZSC/quartz, (b) SDS/quartz.

slope, respectively. Reported ranges in adsorption literature indicate that adsorption energies below 8–40 kJ/mol are characteristic of physisorption dominated by weak van der Waals and electrostatic interactions, whereas chemisorption processes typically exceed 40 kJ/mol[97,98]. The fitting of adsorption data to the Temkin model is depicted in Fig. 11.

The parameters of Langmuir, Freundlich, and Temkin isotherm models and coefficient of determination (R^2) values obtained by experimental data are reported in Table 3 for the ZSC and SDS surfactants adsorption onto the surface of quartz adsorbent. Parameter R^2 is defined as follows[19]:

$$R^2 = 1 - \frac{\sum_{i=1}^{N} (q_{e,i} - q_{p,i})^2}{\sum_{i=1}^{N} (q_{p,i} - \overline{q_{e,i}})^2} \tag{9}$$

where $q_{e,i}$ and $q_{p,i}$ represent the experimental and predicted equilibrium adsorption values, respectively.

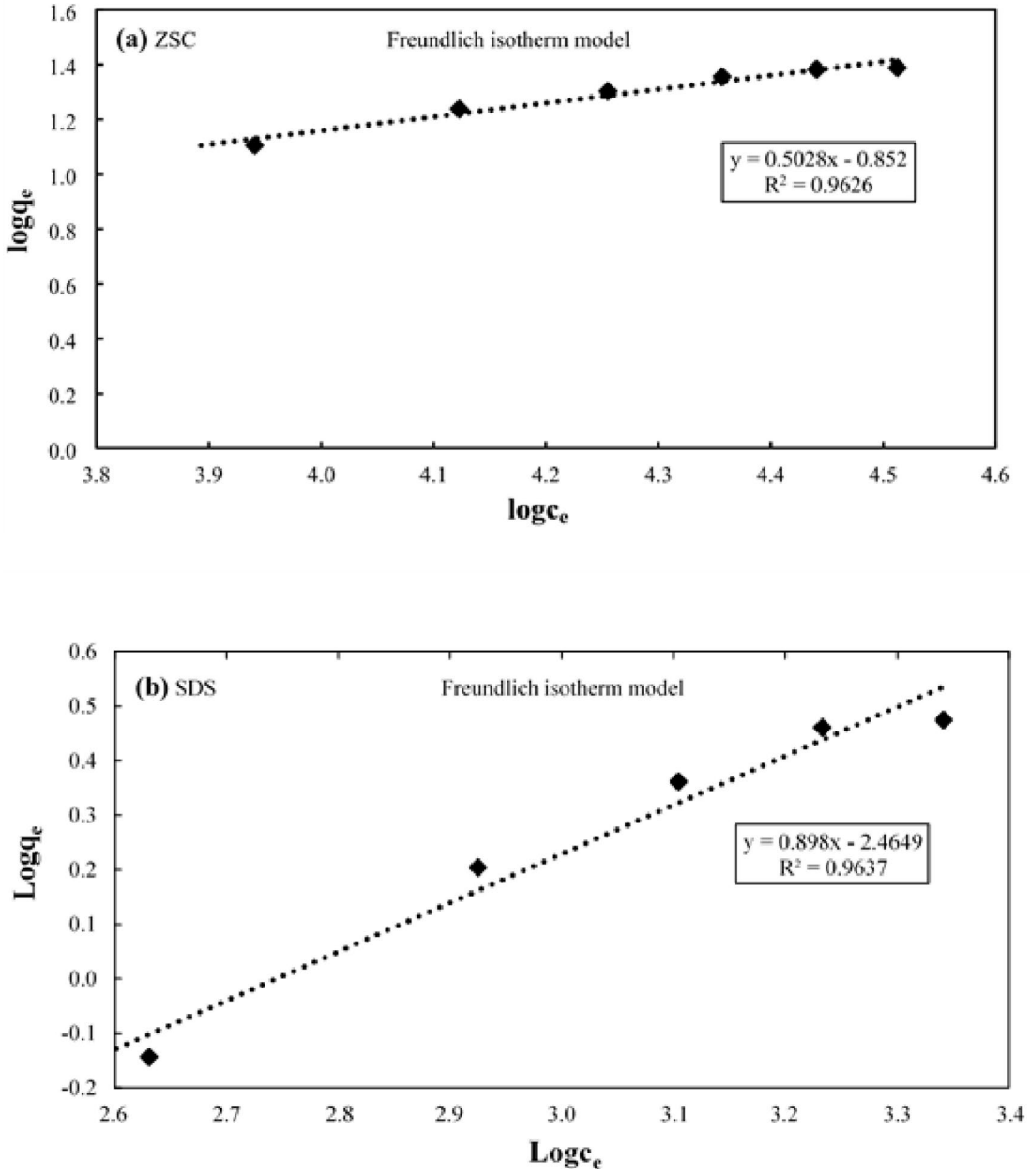

Fig. 10. Freundlich adsorption isotherms fitting curves for (a) ZSC/quartz, (b) SDS/quartz.

The Langmuir model with R^2 = 0.9917 showed the best fit to the experimental data, indicating a uniform monolayer adsorption of surfactant on the homogeneous surface of the adsorbent. The Freundlich model also provides a good fit to the data with an acceptable coefficient of determination (R^2 = 0.9626) and indicates the presence of a heterogeneous surface in the adsorption process. While values of 1/n greater than 1 represent weak adsorption, values of *1/n* between 0.1 and 0.5 demonstrate strong adsorption, and values between 0.5 and 1 denote somewhat difficult adsorption. The value *1/n* = 0.5028, which is in the range of 0.5 to 1, indicates favorable adsorption conditions at different points on the adsorbent surface. Also, the value of k_f = 0.14 indicates the intensity of adsorption at low concentrations. In the Tamkin model, the value of R^2 = 0.9845 also shows a good fit. The parameter b = 268.491 J/mol in this model indicates that the adsorption mechanism is of a physical type, since this value is less than 8000 J/mol and therefore refers to physical bonds[99]. The value of k_t = 4.79×10^{-4} L/mg indicates the relative binding strength between the adsorbent and the adsorbate. Accordingly, it can be concluded that although the Langmuir model has shown the highest accuracy, the Freundlich and Temkin models also provide useful information about the surface heterogeneity and multilayer adsorption, which is essential in a more comprehensive analysis of the adsorption behavior. In particular, the low value of the parameter *1/n* in the Freundlich model and b in the Temkin model can confirm that the adsorption process of ZSC on quartz is influenced by weak bonds between the surfactant and the rock surfaces and that multilayer physical adsorption has occurred on the heterogeneous surface. Also, considering the need to use

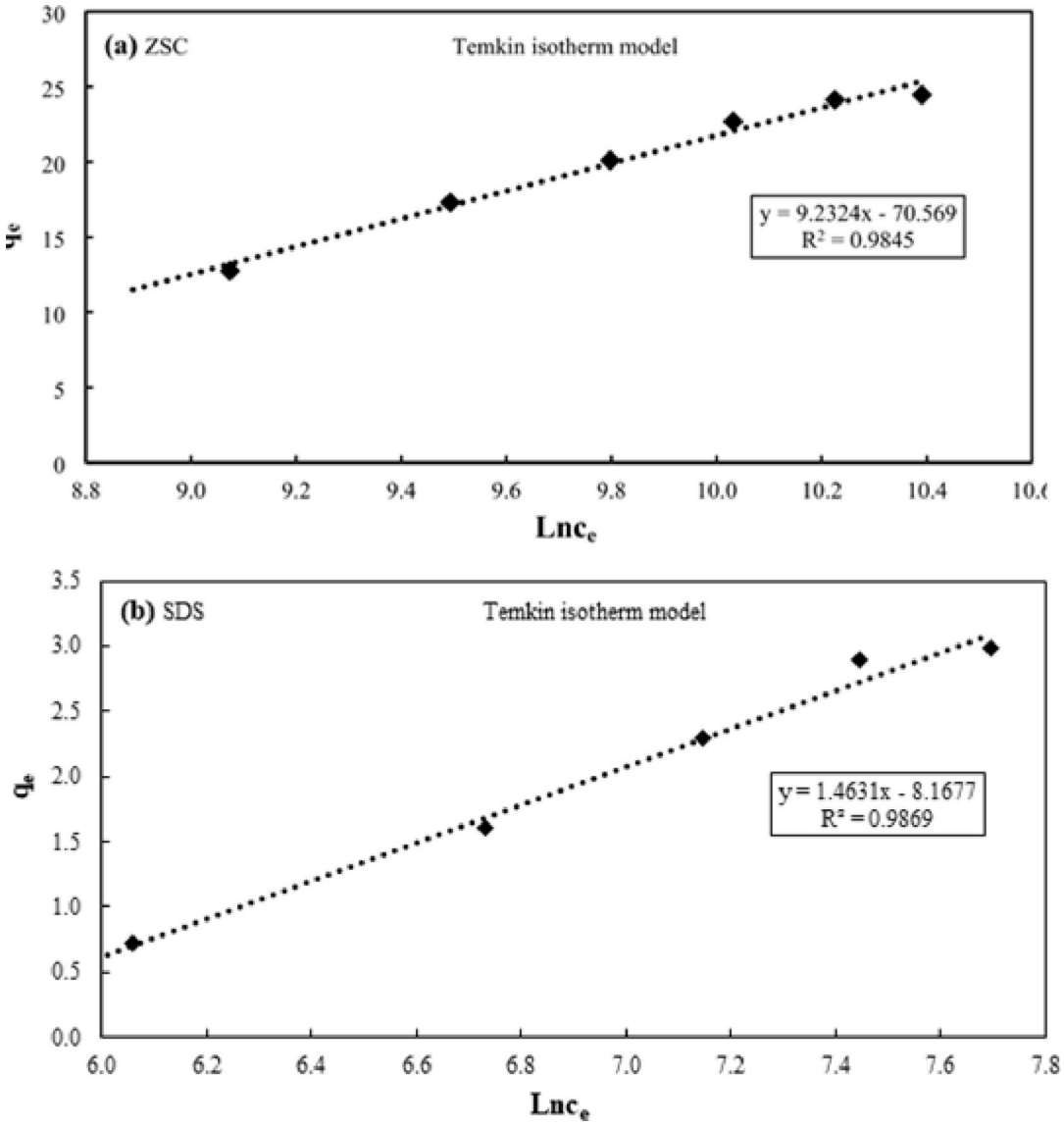

Fig. 11. Temkin adsorption isotherms fitting curves for (a) ZSC/quartz, (b) SDS/quartz.

higher concentrations of natural surfactants in industrial processes, the Freundlich and Temkin models can provide a more accurate description of the adsorption behavior in operational ranges.

According to Table 3, the Langmuir model with a high coefficient of determination ($R^2 = 0.9858$) showed the best fit to the experimental data. This indicates that the adsorption of SDS on quartz surfaces occurs in a monolayer form. The value of R_L = 0.0016 between 0 and 1, indicating the favorable nature of the adsorption based on the Langmuir model. This very low value of R_L indicates that the adsorption was very suitable and effective at the tested concentrations. The Freundlich model, with a relatively lower coefficient of determination ($R^2 = 0.9637$), provided a poorer fit to the data than the Langmuir model. However, the value of $1/n = 0.8980$, which is close to 1, indicates that the adsorbent surface behaves relatively uniformly and the adsorption occurs under near-linear conditions. The very low value of k_f = 0.0034 indicates that the adsorption intensity is very limited at low concentrations of SDS on quartz. In the Temkin model, a relatively high value of $R^2 = 0.9869$ is obtained, indicating that this model also fits the data well. The value of $b = 1694.2$ J/mol, which, considering the value of less than 8000 J/mol, can be concluded that the adsorption mechanism is physical. The value of k_t = 0.0038 L/mg indicates a low strength of interaction between SDS and the quartz surface. Overall, the Langmuir model is the dominant model in describing the adsorption behavior of SDS on quartz due to its higher correlation and significant adsorption capacity. However, the Tamkin model can provide useful information regarding the physical nature of the adsorption process. The Freundlich model provides a weaker description of the adsorption process.

	Models	Parameter	Absorbent Quartz
ZSC	Langmuir	k_l (L/mg)	0.0878
		R_L	0.0011
		R^2	0.9917
	Freundlich	k_f	0.14
		1/n	0.5028
		R^2	0.9626
	Temkin	b(J/mol)	268.491
		k_t (L/mg)	4.79×10^{-4}
		R^2	0.9845
SDS	Langmuir	k_l (L/mg)	0.2468
		R_L	0.0016
		R^2	0.9858
	Freundlich	k_f	0.0034
		1/n	0.8980
		R^2	0.9637
	Temkin	b(J/mol)	1694.2
		k_t(L/mg)	0.0038
		R^2	0.9869

Table 3. Parameters of adsorption isotherm models of ZSC and SDS on quartz.

Conclusions

From the results of this study, it can be concluded that the adsorption of ZSC on quartz (approximately 25 mg/g) is about 8 times more than that of SDS on quartz (around 3 mg/g). The reason is that ZSC is neutral, and it therefore does not repel the negatively charged quartz surface. Based on the correlation coefficient (R^2), the Langmuir model with $R^2 = 0.9917$ for ZSC and $R^2 = 0.9858$ for SDS is the most appropriate model. This study was conducted using pure quartz in order to isolate the fundamental adsorption behavior on the dominant sandstone mineral. It is acknowledged that many sandstone reservoirs contain clay constituents that may enhance surfactant adsorption through specific surface interactions. Therefore, the present results are most representative of quartz-rich systems, and future studies will extend this work to clay-bearing sandstones.

Data availability

The datasets generated during and/or analysed during the current study are available from the corresponding author on reasonable request.

Received: 12 October 2025; Accepted: 6 February 2026
Published online: 09 February 2026

References

1. Belhaj, A., Singh, N. & Sarma, H. Critical assessment of the hybrid impact of surfactants on modified salinity water flooding. *SPE Can. Energy Technol. Conf.* **D022S007** (SPE), R001. https://doi.org/10.2118/208974-MS (2022).
2. Ghatee, A. & Zarrinpoor, N. Designing an oil supply chain network considering sustainable development paradigm and uncertainty. *Chem. Eng. Res. Des.* **184**, 692–723 (2022).
3. Laben, A. B. et al. Experimental study on the performance of emulsions produced during ASP flooding. *J. Pet. Explor. Prod. Technol.* **12**, 1797–1809 (2022).
4. Norouzpour, M. et al. Red beet plant as a novel source of natural surfactant combined with 'Smart water' for EOR purposes in carbonate reservoirs. *J. Mol. Liq.* **370**, 121051 (2023).
5. Pal, N., Babu, K. & Mandal, A. Surface tension, dynamic light scattering and rheological studies of a new polymeric surfactant for application in enhanced oil recovery. *J. Pet. Sci. Eng.* **146**, 591–600 (2016).
6. Pal, N., Kumar, N., Verma, A., Ojha, K. & Mandal, A. Performance evaluation of novel sunflower oil-Based gemini Surfactant(s) with different spacer lengths: application in enhanced oil recovery. *Energy Fuels.* **32**, 11344–11361 (2018).
7. Atta, D. Y., Negash, B. M., Yekeen, N. & Habte, A. D. A state-of-the-art review on the application of natural surfactants in enhanced oil recovery. *J. Mol. Liq.* **321**, 114888 (2021).
8. Hosseini, H., Apourvari, S. N. & Schaffie, M. Wettability alteration of carbonate rocks via magnetic fields application. *J. Pet. Sci. Eng.* **172**, 280–287 (2019).
9. Barari, M., Lashkarbolooki, M., Abedini, R. & Hezave, A. Z. Effects of conventional and ionic liquid-based surfactants and sodium tetraborate on interfacial tension of acidic crude oil. *Sci. Rep.* **14**, 2618 (2024).
10. Abhishek, R., Kumar, G. S. & Sapru, R. K. Wettability alteration in carbonate reservoirs using nanofluids. *Pet. Sci. Technol.* **33**, 794–801 (2015).
11. Mandal, A. & Ojha, K. *Enhanced Oil Recovery*CRC Press,. at (2023). https://www.taylorfrancis.com/books/9781003098850
12. Bahraminejad, H., K Manshad, A., Iglauer, S. & Keshavarz, A. NEOR mechanisms and performance analysis in carbonate/sandstone rock coated microfluidic systems. *Fuel* **309**, 122327 (2022).
13. Shehzad, F. et al. Polymeric surfactants and emerging alternatives used in the demulsification of produced water: A review. *Polym. Rev.* **58**, 63–101 (2018).

14. Shakeel, M., Samanova, A., Pourafshary, P. & Hashmet, M. R. Experimental analysis of oil displacement by hybrid engineered water / chemical EOR approach in carbonates. *J. Pet. Sci. Eng.* **207**, 109297 (2021).
15. Nafisifar, A., Khaksar Manshad, A. & Reza Shadizadeh, S. Evaluation of a new green synthesized surfactant from linseeds - chemical EOR implications from sandstone petroleum reservoirs. *J. Mol. Liq.* **342**, 117263 (2021).
16. Bahraminejad, H., Manshad, A. K., Keshavarz, A. & Characterization Micellization Behavior, and performance of a novel surfactant derived from Gundelia tournefortii plant during chemical enhanced oil recovery. *Energy Fuels*. **35**, 1259–1272 (2021).
17. Khayati, H., Moslemizadeh, A., Shahbazi, K., Moraveji, M. K. & Riazi, S. H. An experimental investigation on the use of saponin as a non-ionic surfactant for chemical enhanced oil recovery (EOR) in sandstone and carbonate oil reservoirs: IFT, wettability alteration, and oil recovery. *Chem. Eng. Res. Des.* **160**, 417–425 (2020).
18. Manshad, A. K., Ali, J. A., Haghighi, O. M., Sajadi, M., Keshavarz, A. & S. & Oil recovery aspects of ZnO/SiO_2 nano-clay in carbonate reservoir. *Fuel* **307**, 121927 (2022).
19. Aghamohammadi, N., Schaffie, M., Ranjbar, M. & Zabihi, R. Investigating the impact of Bacillus subtilis bioproducts on static adsorption of asphaltene on dolomite and calcite. *Fuel* **397**, 135240 (2025).
20. Ebrahimi, M., Ghalenavi, H., Schaffie, M., Ranjbar, M. & Hemmati-Sarapardeh, A. Toward mechanistic Understanding of wettability alteration in carbonate rocks in the presence of nanoparticles, gelatin biopolymer, and core-shell nanocomposite of Fe_3O_4@gelatin. *Sci. Rep.* **14**, 31679 (2024).
21. Ghalenavi, H., Hemmati-Sarapardeh, A., Schaffie, M. & Norouzi-Apourvari, S. Application of synthesized Fe_3O_4@Gelatin nanoparticles on interfacial properties and enhanced oil recovery. *Sci. Rep.* **15**, 2558 (2025).
22. Hirasaki, G. J., Miller, C. A. & Puerto, M. Recent advances in surfactant EOR. *SPE J.* **16**, 889–907 (2011).
23. Hosseini, H. et al. Static adsorption and interfacial tension of sodium Dodecyl sulfate via magnetic field application. *J. Pet. Sci. Eng.* **178**, 205–215 (2019).
24. Nowrouzi, I., Manshad, A. K. & Mohammadi, A. H. Evaluation of interfacial tension (IFT), oil swelling and oil production under imbibition of carbonated water in carbonate oil reservoirs. *J. Mol. Liq.* **312**, 113455 (2020).
25. Kamkar, A., Hosseini, H., Norouzi-Apourvari, S. & Schaffie, M. Insight into the synergic effect of ultrasonic Waves, SDS Surfactant, and silica nanoparticles on wettability alteration of carbonate rocks. *Arab. J. Sci. Eng.* **47**, 11609–11622 (2022).
26. Riswati, S. S. et al. Surfactant technology for improved hydrocarbon recovery in unconventional liquid reservoirs: a systematic literature review. *IOP Conf. Ser. Earth Environ. Sci.* **1239**, 012039 (2023).
27. Abbas, A. H., Alsaheb, A., Abdullah, J. K. & R. A. & Comparative study of natural chemical for enhanced oil recovery: focus on extraction and adsorption at quartz sand surface. *Petroleum* **9**, 83–93 (2023).
28. Nieto-Alvarez, D. A. et al. Static and dynamic adsorption of supramolecular surfactant for oil recovery in high temperature and salinity conditions. *J. Surfactants Deterg.* **26**, 817–826 (2023).
29. Holmberg, K. Natural surfactants. *Curr. Opin. Colloid Interface Sci.* **6**, 148–159 (2001).
30. Daghlian Sofla, S. J., Sharifi, M. & Hemmati Sarapardeh, A. Toward mechanistic Understanding of natural surfactant flooding in enhanced oil recovery processes: the role of salinity, surfactant concentration and rock type. *J. Mol. Liq.* **222**, 632–639 (2016).
31. Rodríguez-Cruz, M. S., Sanchez-Martin, M. J. & Sanchez-Camazano, M. A comparative study of adsorption of an anionic and a non-ionic surfactant by soils based on physicochemical and mineralogical properties of soils. *Chemosphere* **61**, 56–64 (2005).
32. Sánchez-Martín, M. J., Dorado, M. C., del Hoyo, C. & Rodríguez-Cruz, M. S. Influence of clay mineral structure and surfactant nature on the adsorption capacity of surfactants by clays. *J. Hazard. Mater.* **150**, 115–123 (2008).
33. Zhu, L. & Feng, S. Synergistic solubilization of polycyclic aromatic hydrocarbons by mixed anionic–nonionic surfactants. *Chemosphere* **53**, 459–467 (2003).
34. Wu, Y. et al. Reducing surfactant adsorption on rock by silica nanoparticles for enhanced oil recovery. *J. Pet. Sci. Eng.* **153**, 283–287 (2017).
35. Herawati, I., Permadi, P., Rochliadi, A. & Marhaendrajana, T. Adsorption of anionic surfactant on sandstone reservoir containing clay minerals and its effect on wettability alteration. *Energy Rep.* **8**, 11554–11568 (2022).
36. Belhaj, A. F. et al. Static adsorption evaluation for anionic-nonionic surfactant mixture on sandstone in the presence of crude oil at high reservoir temperature condition. *SPE Reserv. Eval Eng.* **25**, 261–272 (2022).
37. Belhaj, A. F. & R044 (SPE. Surfactant Partitioning and Adsorption in Chemical EOR: The Neglected Phenomenon in Porous Media. in *SPE/IATMI Asia Pacific Oil Gas Conf. Exhib.* D012S032, at (2021). https://onepetro.org/SPEAPOG/proceedings/21APOG/21APOG/D012S032R044/470086
38. Belhaj, A. F. et al. Experimental investigation, binary modelling and artificial neural network prediction of surfactant adsorption for enhanced oil recovery application. *Chem. Eng. J.* **406**, 127081 (2021).
39. Lebouachera, S. E. I. et al. Experimental investigations of SDS adsorption on the Algerian rock reservoir: chemical enhanced oil recovery case. *Res. Chem. Intermed.* **44**, 7665–7690 (2018).
40. Ahmadi, M. A. & Shadizadeh, S. R. Experimental investigation of adsorption of a new nonionic surfactant on carbonate minerals. *Fuel* **104**, 462–467 (2013).
41. Zendehboudi, S., Ahmadi, M. A., Rajabzadeh, A. R., Mahinpey, N. & Chatzis, I. Experimental study on adsorption of a new surfactant onto carbonate reservoir samples—application to EOR. *Can. J. Chem. Eng.* **91**, 1439–1449 (2013).
42. Somasundaran, P. & Zhang, L. Adsorption of surfactants on minerals for wettability control in improved oil recovery processes. *J. Pet. Sci. Eng.* **52**, 198–212 (2006).
43. Gbadamosi, A. O., Junin, R., Manan, M. A., Agi, A. & Yusuff, A. S. An overview of chemical enhanced oil recovery: recent advances and prospects. *Int. Nano Lett.* **9**, 171–202 (2019).
44. Yekeen, N., Manan, M. A., Idris, A. K. & Samin, A. M. Influence of surfactant and electrolyte concentrations on surfactant adsorption and foaming characteristics. *J. Pet. Sci. Eng.* **149**, 612–622 (2017).
45. Ma, K. et al. Adsorption of cationic and anionic surfactants on natural and synthetic carbonate materials. *J. Colloid Interface Sci.* **408**, 164–172 (2013).
46. Amirianshoja, T., Junin, R., Kamal Idris, A. & Rahmani, O. A comparative study of surfactant adsorption by clay minerals. *J. Pet. Sci. Eng.* **101**, 21–27 (2013).
47. Bera, A., Kumar, T., Ojha, K. & Mandal, A. Adsorption of surfactants on sand surface in enhanced oil recovery: Isotherms, kinetics and thermodynamic studies. *Appl. Surf. Sci.* **284**, 87–99 (2013).
48. Belhaj, A. F., Elraies, K. A., Shuhili, J. A., Mahmood, S. M. & Tewari, R. D. Surfactant adsorption evaluation in the presence of crude oil at high reservoir temperature condition. in *Offshore Technol. Conf. Asia* **D011S008R001** (OTC, (2020).
49. Belhaj, A. F. et al. Partitioning behaviour of novel surfactant mixture for high reservoir temperature and high salinity conditions. *Energy* **198**, 117319 (2020).
50. Belhaj, A. F., Fakir, S. H., Javadi, A. H. & Sarma, H. K. Bridging Laboratory Insights to Field Applications: Advancing Geochemical Modelling of Hybrid Low-Salinity Surfactant Flooding in Carbonates. in *SPE Annu. Tech. Conf. Exhib.* D011S009R004SPE, (2025).
51. Machale, J., Majumder, S. K., Ghosh, P., Sen, T. K. & Saeedi, A. Impact of mineralogy, salinity, and temperature on the adsorption characteristics of a novel natural surfactant for enhanced oil recovery. *Chem. Eng. Commun.* **209**, 143–157 (2022).
52. Ebrahimi, M., Ghalenavi, H., Schaffie, M., Ranjbar, M. & Hemmati-Sarapardeh, A. Experimental investigation of wettability alteration in sandstone rock by nanoparticles, gelatin biopolymer, salt ions, and synthesized Fe_3O_4/gelatin nanocomposite for EOR applications. *Sci. Rep.* **15**, 33260 (2025).
53. Pal, N., Saxena, N., Laxmi, K. V. D. & Mandal, A. Interfacial behaviour, wettability alteration and emulsification characteristics of a novel surfactant: implications for enhanced oil recovery. *Chem. Eng. Sci.* **187**, 200–212 (2018).

54. Ahmadi, M. A. & Shadizadeh, S. R. Experimental investigation of a natural surfactant adsorption on shale-sandstone reservoir rocks: static and dynamic conditions. *Fuel* **159**, 15–26 (2015).
55. Ahmadi, M. A., Zendehboudi, S., Shafiei, A. & James, L. Nonionic surfactant for enhanced oil recovery from carbonates: adsorption kinetics and equilibrium. *Ind. Eng. Chem. Res.* **51**, 9894–9905 (2012).
56. Bozicevic, A., De Mieri, M., Di Benedetto, A., Gafner, F. & Hamburger, M. Dammarane-type saponins from leaves of Ziziphus spina-christi. *Phytochemistry* **138**, 134–144 (2017).
57. Singh, D. & Chaudhuri, P. K. Structural characteristics, bioavailability and cardioprotective potential of saponins. *Integr. Med. Res.* **7**, 33–43 (2018).
58. Hostettmann, K., Marston, A. & Saponins *(No Title)* 1 (1995).
59. Emadi, S. et al. Effect of using zyziphus spina Christi or Cedr extract (CE) as a natural surfactant on oil mobility control by foam flooding. *J. Mol. Liq.* **293**, 111573 (2019).
60. Arabloo, M., Ghazanfari, M. H. & Rashtchian, D. Wettability modification, interfacial tension and adsorption characteristics of a new surfactant: implications for enhanced oil recovery. *Fuel* **185**, 199–210 (2016).
61. Summerton, E. et al. The impact of N,N-dimethyldodecylamine N-oxide (DDAO) concentration on the crystallisation of sodium Dodecyl sulfate (SDS) systems and the resulting changes to crystal structure, shape and the kinetics of crystal growth. *J. Colloid Interface Sci.* **527**, 260–266 (2018).
62. Ghosh, B. & Li, X. Effect of surfactant composition on reservoir wettability and scale inhibitor squeeze lifetime in oil wet carbonate reservoir. *J. Pet. Sci. Eng.* **108**, 250–258 (2013).
63. López-Díaz, D. & Velázquez, M. M. Variation of the critical micelle concentration with surfactant structure: a simple method to analyze the role of attractive–repulsive forces on micellar association. *Chem. Educ.* **12**, 327–330 (2007).
64. Ezeonyeka, N. L., Hemmati-Sarapardeh, A. & Husein, M. M. Asphaltenes adsorption onto metal oxide nanoparticles: A critical evaluation of measurement techniques. *Energy Fuels.* **32**, 2213–2223 (2018).
65. Stuart, B. H. *Infrared Spectroscopy: Fundamentals and Applications* (Wiley, 2004). https://onlinelibrary.wiley.com/doi/book/10.1002/0470011149%3Eat <
66. Stuart, B. in *Kirk-Othmer Encycl. Chem. Technol.*Wiley, at https://onlinelibrary.wiley.com/doi/ (2005). https://doi.org/10.1002/0471238961.0914061810151405.a01.pub2%3E
67. Soleimani, Y., Mohammadi, M. R., Schaffie, M., Zabihi, R. & Ranjbar, M. An experimental study of the effects of bacteria on asphaltene adsorption and wettability alteration of dolomite and quartz. *Sci. Rep.* **13**, 21497 (2023).
68. Zargartalebi, M., Kharrat, R. & Barati, N. Enhancement of surfactant flooding performance by the use of silica nanoparticles. *Fuel* **143**, 21–27 (2015).
69. Hollander, A. F., Somasundaran, P. & Gryte, C. C. in *Adsorpt. from Aqueous Solut.* 143–162Springer, (1981).
70. Somasundaran, P. & Agar, G. The zero point of charge of calcite. *J. Colloid Interface Sci.* **24**, 433–440 (1967).
71. Kumar, N. & Mandal, A. Wettability alteration of sandstone rock by surfactant stabilized nanoemulsion for enhanced oil recovery—A mechanistic study. *Colloids Surf. Physicochem Eng. Asp.* **601**, 125043 (2020).
72. Babu, K., Pal, N., Bera, A., Saxena, V. K. & Mandal, A. Studies on interfacial tension and contact angle of synthesized surfactant and polymeric from castor oil for enhanced oil recovery. *Appl. Surf. Sci.* **353**, 1126–1136 (2015).
73. Bera, A., Ojha, S. K., Kumar, K., Mandal, A. & T. & Mechanistic study of wettability alteration of quartz surface induced by nonionic surfactants and interaction between crude oil and quartz in the presence of sodium chloride salt. *Energy Fuels.* **26**, 3634–3643 (2012).
74. KJELLIN, M. & JOHANSSON, I. A. R. D. *Surfactants from Renewable Resources* (Wiley, 2010). https://doi.org/10.1002/9780470686607
75. SHAH, S. S. & KHAN, A. M. Determination of critical micelle concentration (Cmc) of sodium Dodecyl sulfate (SDS) and the effect of low concentration of pyrene on its Cmc using ORIGIN software. *J. Chem. Soc. Pakistan.* **30**, 186 (2011).
76. Barati-Harooni, A., Najafi-Marghmaleki, A., Tatar, A. & Mohammadi, A. H. Experimental and modeling studies on adsorption of a nonionic surfactant on sandstone minerals in enhanced oil recovery process with surfactant flooding. *J. Mol. Liq.* **220**, 1022–1032 (2016).
77. Sen Gupta, S. & Bhattacharyya, K. G. Immobilization of Pb(II), Cd(II) and Ni(II) ions on kaolinite and montmorillonite surfaces from aqueous medium. *J. Environ. Manage.* **87**, 46–58 (2008).
78. Saxena, N., Kumar, A. & Mandal, A. Adsorption analysis of natural anionic surfactant for enhanced oil recovery: the role of mineralogy, salinity, alkalinity and nanoparticles. *J. Pet. Sci. Eng.* **173**, 1264–1283 (2019).
79. DİKMEN, S., ERSOY, B., DİKMEN, Z., ADSORPTION BEHAVIOUR OF IONIC AND NON-IONIC SURFACTANTS ONTO TALC & A NATURALLY HYDROPHOBIC MINERAL-A COMPARATIVE STUDY. *Eskişehir Tech. Univ. J. Sci. Technol. - Appl. Sci. Eng.* **21**, 139–152 (2020).
80. Das, D., Panigrahi, S., Misra, P. K. & Nayak, A. Effect of organized Assemblies. Part 4. Formulation of highly concentrated Coal–Water slurry using a natural surfactant. *Energy Fuels.* **22**, 1865–1872 (2008).
81. Zhang, L., Somasundaran, P., Mielczarski, J. & Mielczarski, E. Adsorption mechanism of n-dodecyl-β-D-maltoside on alumina. *J. Colloid Interface Sci.* **256**, 16–22 (2002).
82. James, R. O. & Healy, T. W. Adsorption of hydrolyzable metal ions at the oxide—water interface. III. A thermodynamic model of adsorption. *J. Colloid Interface Sci.* **40**, 65–81 (1972).
83. Yusuf, M., Wathon, M. H., Thanasaksukthawee, V., Saul, A. & Tangparitkul, S. Adsorption of saponin natural surfactant on carbonate rock and comparison to synthetic surfactants: an enhanced oil recovery prospective. *Energy Fuels.* **35**, 11193–11202 (2021).
84. Dauyltayeva, A. et al. Screening of chemicals to enhance oil recovery in a mature sandstone oilfield in kazakhstan: overcoming challenges of high residual oil. *Appl. Sci.* **13**, 10307 (2023).
85. Zulkifli, N. N. et al. Evaluation of new surfactants for enhanced oil recovery applications in high-temperature reservoirs. *J. Pet. Explor. Prod. Technol.* **10**, 283–296 (2020).
86. Belhaj, A. F. et al. The effect of surfactant concentration, salinity, temperature, and pH on surfactant adsorption for chemical enhanced oil recovery: a review. *J. Pet. Explor. Prod. Technol.* **10**, 125–137 (2020).
87. Zhang, L. et al. Static adsorption of a switchable Diamine surfactant on natural and synthetic minerals for high-salinity carbonate reservoirs. *Colloids Surf. Physicochem Eng. Asp.* **583**, 123910 (2019).
88. Bashir, A., Haddad, A. S. & Rafati, R. A review of fluid displacement mechanisms in surfactant-based chemical enhanced oil recovery processes: analyses of key influencing factors. *Pet. Sci.* **19**, 1211–1235 (2022).
89. Abo Gabal, R., Osama, S., Hanafy, N. & Oraby, A. Micellization thermodynamics as a function of the temperature of a cationic zwitterionic Dodecyl phosphocholine and anionic sodium Dodecyl sulfate mixed micelles with fluorometry. *Appl. Phys. A.* **129**, 201 (2023).
90. Paria, S. & Khilar, K. C. A review on experimental studies of surfactant adsorption at the hydrophilic solid–water interface. *Adv. Colloid Interface Sci.* **110**, 75–95 (2004).
91. Hashem, A., Al-Anwar, A., Nagy, N. M., Hussein, D. M. & Eisa, S. Isotherms and kinetic studies on adsorption of Hg(II) ions onto Ziziphus spina-christi L. from aqueous solutions. *Green. Process. Synth.* **5**, 213–224 (2016).
92. Yekeen, N. et al. Impact of nanoparticles–surfactant solutions on carbon dioxide and methane wettabilities of organic-rich shale and CO_2/brine interfacial tension: implication for carbon geosequestration. *Energy Rep.* **8**, 15669–15685 (2022).
93. Zhuravlev, L. T. The surface chemistry of amorphous silica. Zhuravlev model. *Colloids Surf. Physicochem Eng. Asp.* **173**, 1–38 (2000).

94. Kalam, S., Abu-Khamsin, S. A., Kamal, M. S. & Patil, S. Surfactant adsorption isotherms: A review. *ACS Omega*. **6**, 32342–32348 (2021).
95. Liu, Z., Zhao, G., Brewer, M., Lv, Q. & Sudhölter, E. J. R. Comprehensive review on surfactant adsorption on mineral surfaces in chemical enhanced oil recovery. *Adv. Colloid Interface Sci.* **294**, 102467 (2021).
96. Langmuir, I. & THE ADSORPTION OF GASES ON PLANE SURFACES OF GLASS MICA AND PLATINUM. *J. Am. Chem. Soc.* **40**, 1361–1403 (1918).
97. Foo, K. Y. & Hameed, B. H. Insights into the modeling of adsorption isotherm systems. *Chem. Eng. J.* **156**, 2–10 (2010).
98. Ruthven, D. M. *Principles of Adsorption and Adsorption Processes* (Wiley, 1984).
99. Inam, E., Etim, U. J., Akpabio, E. G. & Umoren, S. A. Process optimization for the application of carbon from plantain peels in dye abstraction. *J. Taibah Univ. Sci.* **11**, 173–185 (2017).

Author contributions

Arash Shirali: Investigation, Data curation, Writing original draft, Mohammad Ebrahimi: Investigation, Methodology, Writing original draft, Abdolhossein Hemmati-Sarapardeh: Supervision, Conceptualization, Validation, Visualization, Mohammad Ranjbar: Validation, Visualization, Writing-Review & Editing, Mahin Schaffie: Validation, Methodology, Writing Review & Editing.

Funding

No financial support was received by the authors in this research.

Declarations

Competing interests

The authors declare no competing interests.

Additional information

Correspondence and requests for materials should be addressed to M.E., A.H.-S. or M.S.